technologies

MDPI

Article

Comparison of a Custom-Made Inexpensive Air Permeability Tester with a Standardized Measurement Instrument

Dietrich Spädt [1], Niclas Richter [1], Cornelia Golle [2], Andrea Ehrmann [1,*] and Lilia Sabantina [2,3]

[1] Faculty of Engineering and Mathematics, Bielefeld University of Applied Sciences and Arts, 33619 Bielefeld, Germany; niclas.richter@hsbi.de (N.R.)
[2] Department of Apparel Engineering and Textile Processing, Berlin University of Applied Sciences—HTW Berlin, 12459 Berlin, Germany; lilia.sabantina@htw-berlin.de (L.S.)
[3] Department of Textile and Paper Engineering, Higher Polytechnic School of Alcoy, Polytechnic University of Valencia (UPV), 03801 Alcoy, Spain
* Correspondence: andrea.ehrmann@hsbi.de

Abstract: The air permeability of a textile fabric belongs to the parameters which characterize its potential applications as garments, filters, airbags, etc. Calculating the air permeability is complicated due to its dependence on many other fabric parameters, such as porosity, thickness, weaving parameters and others, which is why the air permeability is usually measured. Standardized measurement instruments according to EN ISO 9237, however, are expensive and complex, prohibiting small companies or many universities from using them. This is why a simpler and inexpensive test instrument was suggested in a previous paper. Here, we show correlations between the results of the standardized and the custom-made instrument and verify this correlation using fluid dynamics calculations.

Keywords: air permeability; fluid dynamics; EN ISO 9237; piston; gravity

check for updates

Citation: Spädt, D.; Richter, N.; Golle, C.; Ehrmann, A.; Sabantina, L. Comparison of a Custom-Made Inexpensive Air Permeability Tester with a Standardized Measurement Instrument. *Technologies* **2024**, *12*, 79. https://doi.org/10.3390/technologies12060079

Academic Editor: Frédéric C. Lebon

Received: 25 April 2024
Revised: 27 May 2024
Accepted: 31 May 2024
Published: 2 June 2024

1. Introduction

Measuring air permeability is important to evaluate whether a textile fabric is suitable for different applications, from clothing to diverse technical textiles [1]. Usually, this value is measured by testing the air flowing through a defined fabric area within a defined time under the impact of a defined pressure (e.g., 100 Pa), a definition which has been used since the middle of the 20th century [2–4]. Test procedures based on this principle are described in several standards with slightly varying parameters, e.g., EN ISO 9237 (Textiles—Determination of Permeability of Fabrics to Air [5]), ASTM D737-75 (Standard Test Method for Air Permeability of Textile Fabrics [6]), or ASTM F778-82 (Standard Methods for Gas Flow Resistance Testing of Filtration Media [7]).

While measurements according to these standards are regularly reported in the recent literature [8–10], the test instruments are relatively expensive and not easy to build, impeding many small companies and research groups from measuring air permeability. An alternative test procedure, which was already suggested in 1932, is based on the principle of a falling cylinder, where a cylinder falls down due to gravity and by this pulls air through textile fabric of a defined area [11]. A slightly different principle was patented by Kawabata, who led a falling piston press air through the specimen under investigation and measured the built-up pressure [12], similar to Wagner and Cain [13] and Wang et al. [14] who also used gravity to move a piston against the air pressure built in a chamber which was closed from the outside by a textile fabric. A slight variation in this principle was suggested by Lyu et al. who described a similar system in which pressure was built up by a pump [15].

Recently, we built an inexpensive air permeability test stand based on the falling piston principle and showed that longer falling times were well correlated with smaller air permeability, as could be expected [16]. However, besides the necessity to regularly add lubricant in order to reduce the friction between the piston and the cylinder in which it is falling, no simple correlation between falling duration and air permeability can be expected. On the other hand, a testing instrument, according to the simple physical idea that increased air flowing through the textile under examination will increase the speed of the falling piston, can be built much more easily than the common instruments according to EN ISO 9237 and would thus enable more companies and research groups to measure air permeability in an inexpensive way. Here, we thus describe recent improvements of the lubricant, give results of a larger test series comparing the custom-built test stand with a commercial air permeability tester, and finally calculate the correlation between the falling duration and the standardized air permeability.

2. Materials and Methods

The custom-made air permeability tester consists of a long transparent tube in which a stainless steel piston (mass 2272 g, diameter 94 mm, height 77 mm) can glide down. The overall mass of the piston can be increased by up to 6 additional weights (232 g each). Gaskets around the piston impede air from flowing between piston and tube; they have to be treated by a lubricant to reduce friction. The time which the piston needs to fall from one inductive sensor (40 cm below the starting position) to the next one (40 cm below the first sensor) is measured.

The upper end of the tube has a round open area (10 cm^2, identical to a value specified in EN ISO 9237) in which the textile fabric under examination can be clamped; the lower end is open. To perform a measurement, the piston is introduced into the tube, the latter is rotated by 180° so that the piston glides to the top where it is hold by an electromagnet, the tube is rotated back, and the electromagnet is switched off to release the piston whose falling duration between both inductive sensors is measured. If a textile fabric with low air permeability is investigated, the reduced pressure above the falling piston will reduce its velocity. A more detailed description of the test stand can be found in Ref. [16]; the test stand is shown in Figure 1. Its working principle is based on the idea that the falling piston drags air through the textile specimen under investigation and uses the underpressure built up by this process to measure the air permeability. Briefly, an open-pore fabric which has maximum air permeability will not build up a partial vacuum and thus not reduce the piston's falling speed, while a nearly completely closed textile fabric will only enable air to penetrate slowly, so that a partial vacuum builds up over the falling piston which will reduce its velocity.

(a) (b)

Figure 1. (**a**) Custom-made air permeability test stand; (**b**) piston with 6 additional weights which can be fixed inside the piston using a screw.

Measurements were performed for 0, 3 and 6 additional weights, respectively. As lubricants, Ballistol universal oil and PTFE spray (both from Ballistol, Aham, Germany) were tested. Each experiment with Ballistol universal oil was performed 10 times, while experiments with PFTE spray were performed 5 times each due to their smaller standard deviations. Generally, a suitable lubricant is necessary to reduce the friction between the gaskets and the tube, while at the same time ensuring air-tight contact between gaskets and tube.

Experiments were performed at 22 °C and a relative humidity of 35–38% as no climatized laboratory was available.

For comparison, the commercial air permeability tester FX 3300 Lab Air IV testing instrument (Textest AG, Schwerzenbach, Switzerland), working according to EN ISO 9237, was used (number of measurements per sample $n = 3$).

The textile fabrics under examination are depicted in Table 1. They were chosen as to represent a broad range of different structures, materials and corresponding air permeabilities. Microscopic images were taken with a digital microscope VHX-970FN (Keyence, Neu-Isenburg, Germany).

Table 1. Textile fabrics under examination. Scale bars are 1 mm.

Sample No.	Microscopic Image	Material/Structure	Mass per Unit Area
1	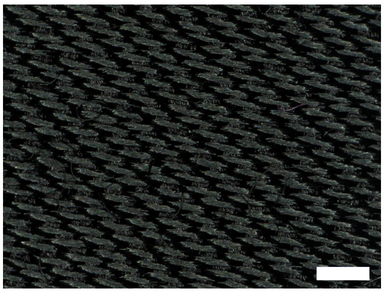	59% virgin wool, 39% viscose, 2% elastane Twill weave	320 g/m^2
2	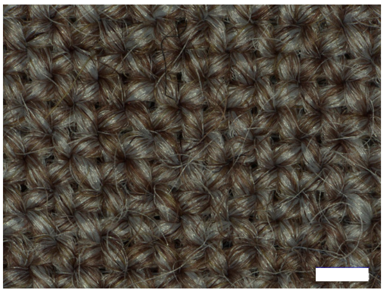	54% polyester, 44% virgin wool, 2% elastane Plain weave	340 g/m^2
3	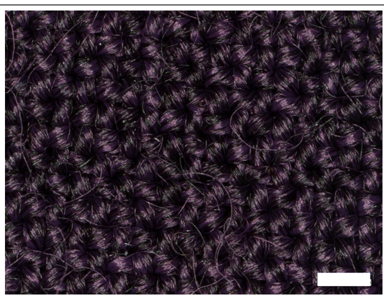	52% polyester, 43% virgin wool, 5% elastane Plain weave	320 g/m^2
4	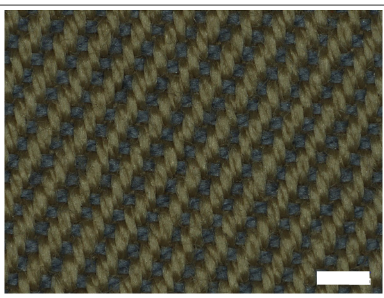	100% cotton Twill weave	300 g/m^2

Table 1. *Cont.*

Sample No.	Microscopic Image	Material/Structure	Mass per Unit Area
5		77% wool, 22% nylon, 1% elastane Plain weave	360 g/m^2
6	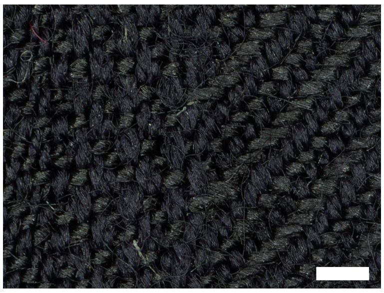	50% cashmere, 15% silk Twill weave	240 g/m^2
7	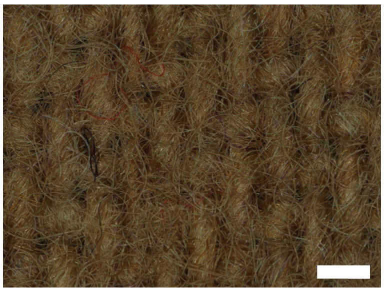	70% wool, 30% polyester Plain weave	350 g/m^2
8	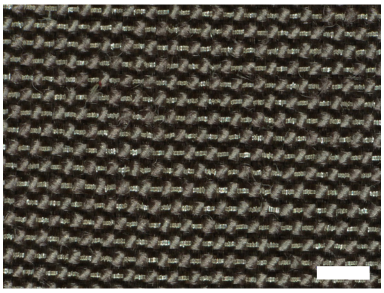	41% polyamide, 59% modal polynosic Plain weave	175 g/m^2
9	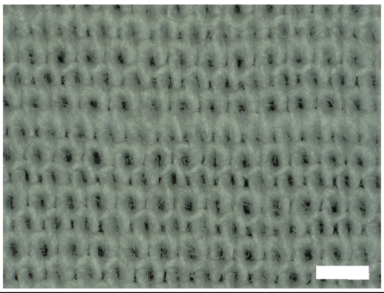	98% cotton, 2% lycra Plain weave	195 g/m^2

Table 1. *Cont.*

Sample No.	Microscopic Image	Material/Structure	Mass per Unit Area
10	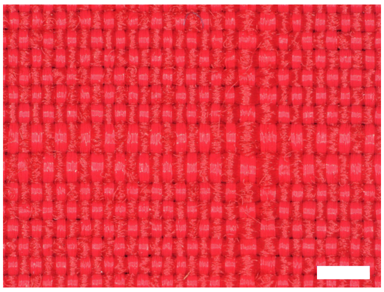	100% polyamide 6.6 Plain weave	188 g/m^2
11	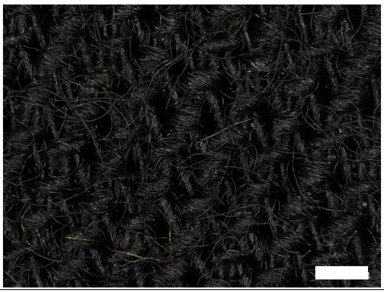	89% virgin wool, 11% polyamide Twill weave	300 g/m^2
12	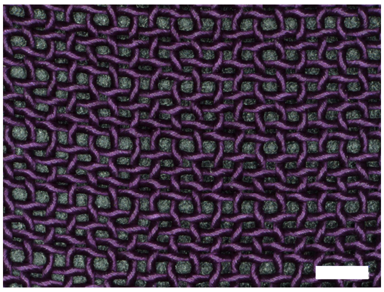	100% viscose Plain weave, Creped fabric	100 g/m^2

3. Results

Firstly, experiments were performed using Ballistol universal oil as lubricant, as in the previous tests [16]. With this lubricant, tests without additional weights were not possible as the piston regularly became stuck in the tube. Figure 2a thus shows only the results with 3 and 6 additional weights, respectively.

In most cases, the error bars (indicating the standard deviations) are relatively small, showing the high reliability of the measurements. The longest time was measured for sample 10, i.e., this sample should have the lowest air permeability, while samples 5 and 12 have the highest air permeability. It must be mentioned here that the air permeability is not directly proportional to the thickness, mass per unit area or the cover factor of a fabric, so that the microscopic images or areal weights in Table 1 cannot be used for a calculation of the air permeability or falling time.

The correlation between measurements with three and with six additional weights is given in Figure 2b. For most measured falling durations, a linear correlation between both values exists; only the longest falling time deviates from this correlation. This can be explained by the slow movement of the gasket through the tube being more influenced by friction, with stick-slip friction as the extreme case; here, apparently the three additional weights are insufficient to fully overcome the friction between gasket and tube.

Next, Figure 3a depicts measurements performed after fully cleaning the whole test stand from Ballistol universal oil and using PTFE spray as a lubricant instead. With this spray, it was also possible to the piston without an additional weight, indicating that PTFE spray can reduce the friction between piston and tube more reliably. Again, sample 10 shows the longest falling time, i.e., the smallest air permeability, again followed by samples 4, 6 and 1. The shortest times, i.e., highest air permeabilities, can again be found for samples 12 and 5. Nevertheless, the ratios between the falling times for different samples or varying numbers of additional weights are different from those measured with Ballistol universal oil. This leads to the question which measurements—with universal oil or with PTFE spray, and with 0, 3, 6 or another number of additional weights—correlates best with the air permeability measured with a standardized testing instrument.

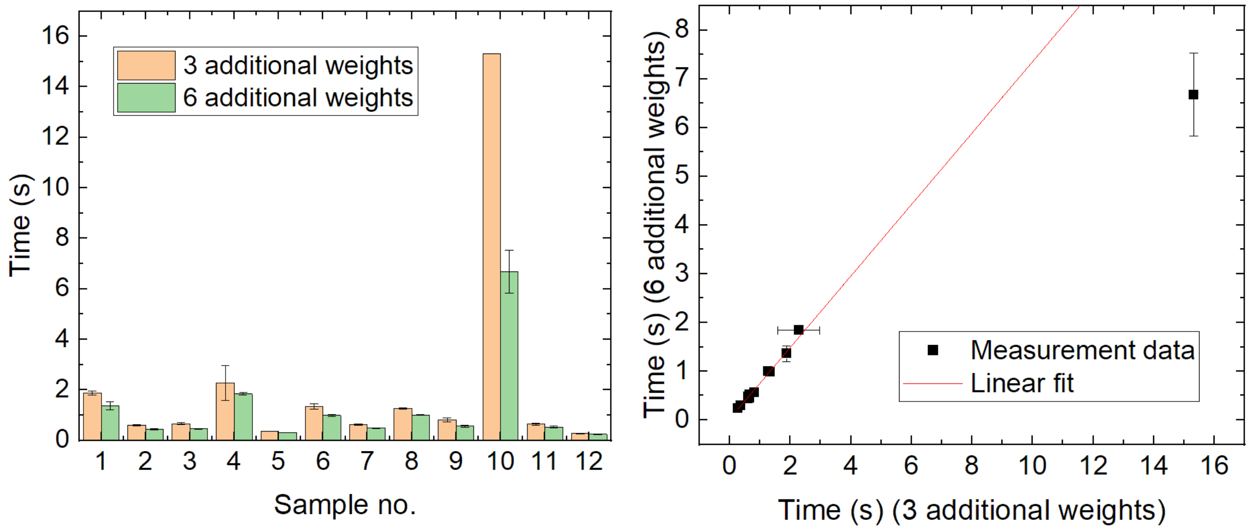

(**a**) (**b**)

Figure 2. (**a**) Measurements with Ballistol universal oil. Error bars show standard deviations. The measurement with 3 additional weights on sample no. 10 could only once be performed since the piston regularly became stuck; (**b**) correlation between Ballistol universal oil measurements with 3 and with 6 additional weights.

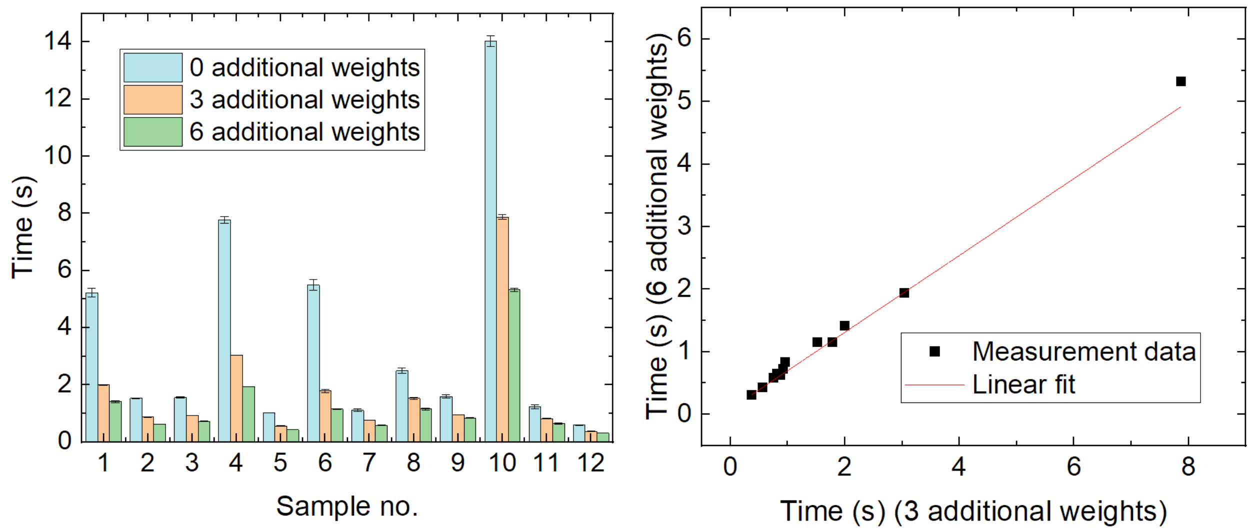

(**a**) (**b**)

Figure 3. (**a**) Measurements with PTFE lubricant; (**b**) correlation between PTFE spray measurements with 3 and with 6 additional weights.

The correlation between measurements with three and with six additional weights for PTFE spray as the lubricant is shown in Figure 3b. Here, the linear correlation also persists for the longest falling time, underlining that PTFE spray leads to more reliable results in a broader range of air permeabilities. The comparison of these values with those taken in measurements without additional weights reveal a much worse correlation, indicating that even with PTFE spray, at least three additional weights should be used.

For the comparison of the values taken with the custom-made air permeability tester, all samples have also been investigated with a commercial air permeability tester according to EN ISO 9237. The results are depicted in Figure 4.

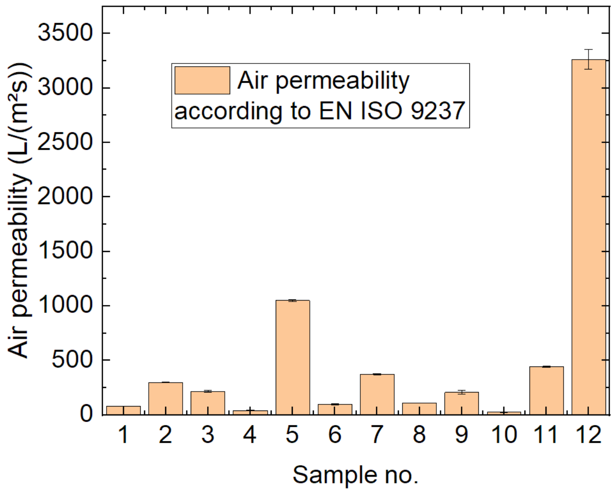

Figure 4. Measurements of the air permeability according to EN ISO 9237.

Figure 5a shows the measured falling times of the custom-made testing instrument vs. the air permeability measured using the standardized testing instrument. Generally, a correlation similar to 1/x is visible, with larger air permeabilities correlated to smaller falling times and vice versa. However, this graph is not suitable to differentiate between 1/x, $1/x^2$ or similar correlations. Figure 5b thus depicts the measured falling times vs. the inverse of the air permeability, as measured using the standardized testing instrument. Here, the measurements with PTFE spray and three or six additional weights especially show an approximately linear correlation, while the measurement with PTFE spray without additional weights shows several outliers, suggesting not using this setup. For the smallest air permeabilities, however, all measured falling times are longer than expected for a simple linear correlation. The next section will thus discuss the correlation between both values, as it can be expected due to fluid dynamic calculations.

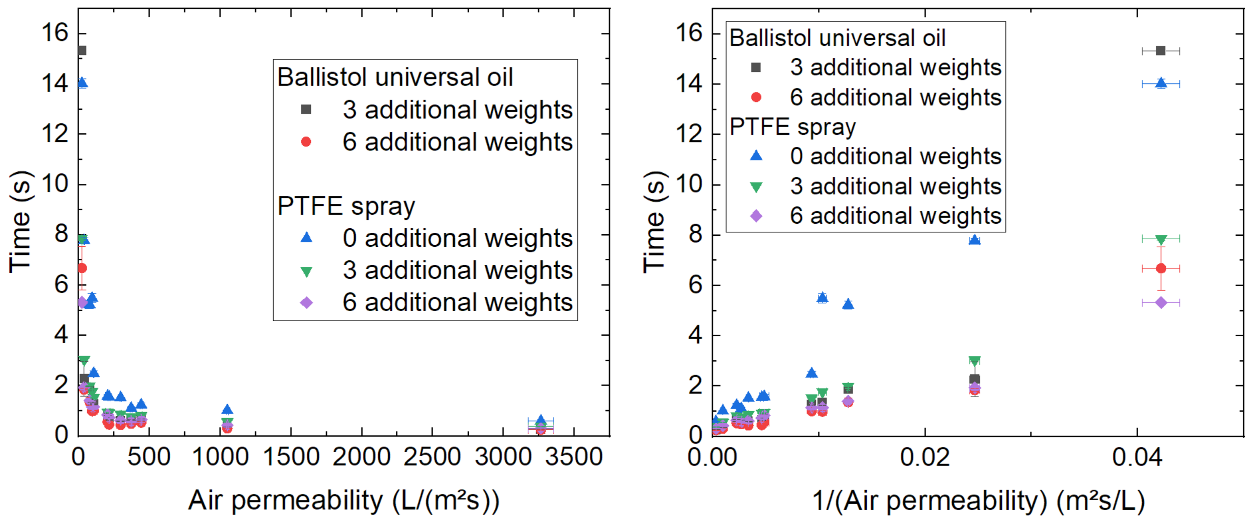

Figure 5. (**a**) Falling time vs. air permeability; (**b**) falling time vs. inverse of the air permeability.

4. Discussion

This section shows a simplified calculation method to estimate the air permeability from the measured falling times.

To transfer the measured values of the custom-made testing device to the commonly used air permeability R of textile fabrics according to EN ISO 9237, a simplified first approach will be shown. The approach presented pursues the goal of firstly calculating the pressure loss coefficient of the inserted sample in terms of plant engineering and pipeline construction. To accomplish this, a couple of assumptions are necessary. Afterwards, by using the same equation as before with different parameters in an imaginary device, one can now calculate the velocity of the airstream perpendicular to the surface of the sample.

The following text uses the simplified test setup shown in Figure 6 to illustrate the calculation method. The whole setup is rotated by 90° for better visibility.

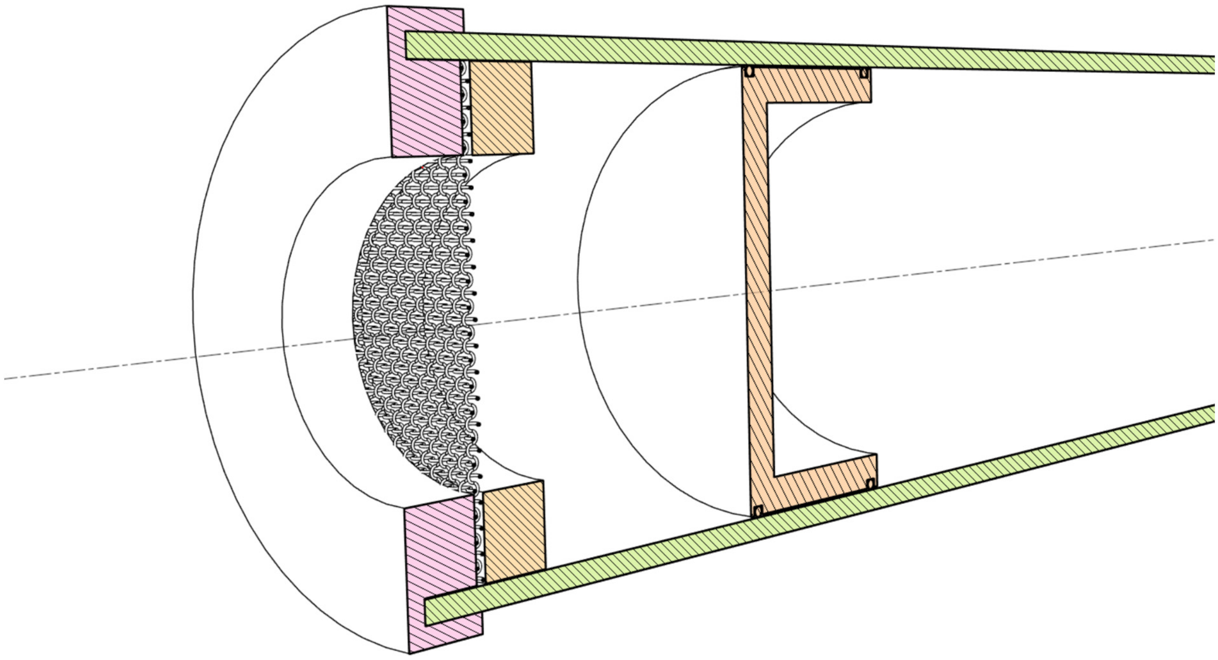

Figure 6. Simplified testing device with a clamped textile fabric (black pattern) and a piston (orange cross-section) in a cylindrical tube (green cross-section).

As already mentioned, the required equations are only valid under certain assumptions which will now be presented. First of all, the friction in two aspects has to be set to zero.

One aspect is the friction between the piston and the cylinder, so that the coefficient of kinetic friction is zero:

$$\mu_k = 0 \tag{1}$$

The second aspect is the inner friction of the fluid so we assume an inviscid flow:

$$\eta = 0 \tag{2}$$

Another property of the fluid is the constant density, so there is no change in space or time:

$$\varrho = const. \tag{3}$$

Furthermore, the piston has to be in force equilibrium ($\sum \vec{F}_{Piston} = 0$), which equals to a constant piston velocity:

$$\vec{v} = const. \tag{4}$$

between the two measurement points where the falling time is measured.

With the assumptions introduced, we are able to estimate the pressure loss coefficient of the sample using the Bernoulli equation including one loss term. Figure 7 includes the necessary quantities in our system and their positions.

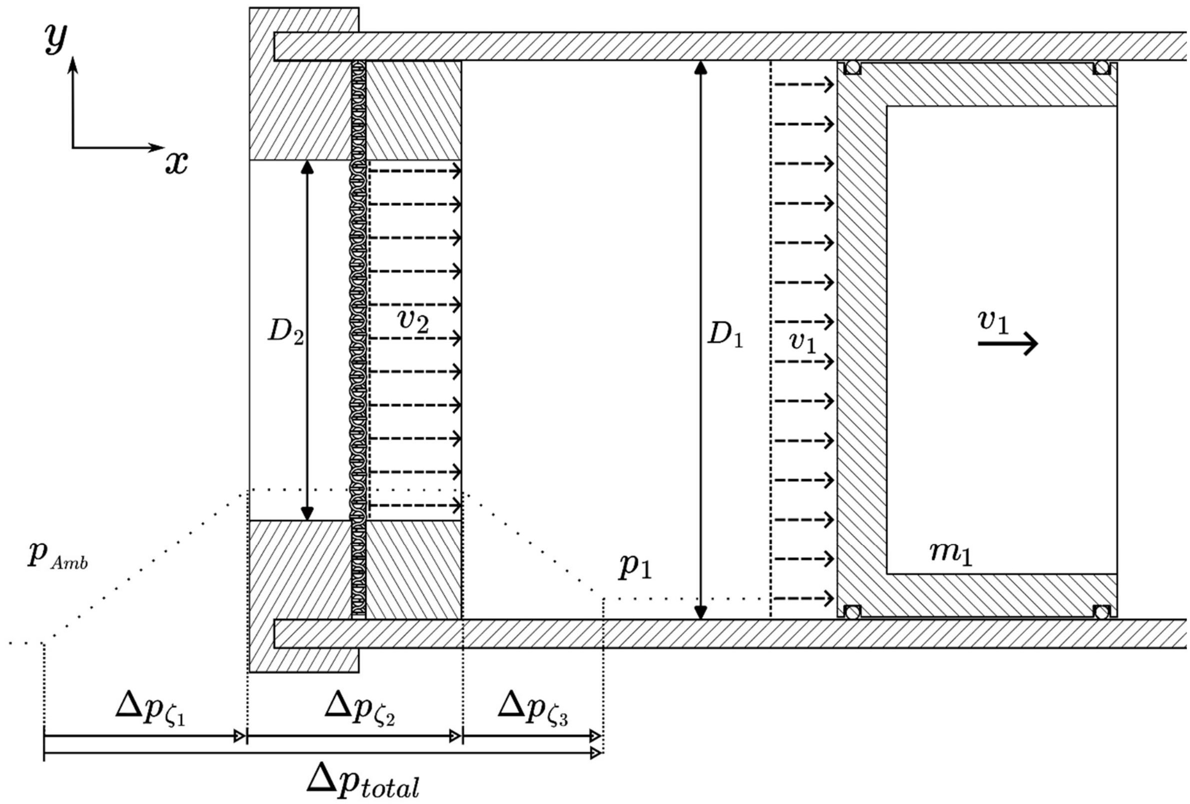

Figure 7. Section view of the system under investigation and relevant quantities. The fabric is the clamped black patterned object on the left side, the piston moves with a velocity v_1 to the right.

As seen in Figure 6, a movement of the piston with mass m_1 in positive x-direction with the velocity v_1 results in fluid flow through the sample inside the chamber between sample and piston. Since we work exclusively with the x component, we do not use vector notation for the velocity or any forces in the following. For simplification, we assume a uniform velocity field over the two relevant diameters, the piston diameter D_1 and the sample diameter D_2. The dashed arrows are intended to represent the velocity field with v_1 for the velocity inside the chamber and v_2 for the velocity at the sample diameter. Because of the uniform velocity field at D_1, the flow velocity is the same as the piston velocity v_1.

The dotted line is an example of a possible streamline and is used in the following. If fluid flows along this dotted line, it has to overcome three main obstacles. Each of these obstacles has its own pressure drop coefficient ζ_i. Two of them are well known and the pressure drop coefficient can be taken from the specialized literature. The first one is the scenario "flow from a tank into a pipe". The pressure drop coefficient for a sharp edge on the inlet side is $\zeta_1 = 0.5$ [17]. The second well known is the Borda–Carnot diffusor, when the fluid leaves the sample holder and the diameter of the cross-section expands from D_2 to D_1. The pressure drop coefficient can be calculated with the following formula [17]:

$$\zeta_3 = \left(1 - \left(\frac{D_2}{D_1}\right)^2\right)^2 \quad (5)$$

The pressure drop over the whole sample holder Δp_{total} can be calculated as mentioned above with the Bernoulli equation including one loss term. Restriction to one loss term is possible, because all terms use the same reference velocity v_2.

$$(p_{Amb} - p_1) = 0.5 \cdot \varrho \cdot v_2^2 \cdot (\zeta_1 + \zeta_2 + \zeta_3) \tag{6}$$

Because of the small difference in height between the two points under consideration, both in the schematic representation and in the real experiment, the energy term based on height difference is neglected. The main target at this point is to separate the pressure drop coefficient ζ_2 for the sample. Rearranging Equation (6) gives the following:

$$\zeta_2 = \frac{(p_{Amb} - p_1)}{0.5 \cdot \varrho \cdot v_2^2} - \zeta_1 - \zeta_3 \tag{7}$$

The unknown quantities are the velocity v_2 and the pressure difference $p_{amb} - p_1$. The flow velocity at the sample can be eliminated by the law of continuity and replacing it with the known piston velocity v_1:

$$v_2 = v_1 \cdot \frac{D_1^2}{D_2^2} \tag{8}$$

Since the piston is in force equilibrium, the gravitational force F_G is equal to the force F_p introduced by the pressure difference between the chamber and the surroundings:

$$F_G + F_p = 0$$

$$F_g = m_1 \cdot g$$

$$F_p = (p_1 - p_{Amb}) \cdot \frac{\pi}{4} \cdot D_1^2$$

These terms can be rearranged to an expression for the pressure difference.

$$F_G = -F_p$$

$$m_1 \cdot g = (p_{Amb} - p_1) \cdot \frac{\pi}{4} \cdot D_1^2$$

$$(p_{Amb} - p_1) = \frac{m_1 \cdot g}{\frac{\pi}{4} \cdot D_1^2} \tag{9}$$

Now the unknown terms in (7) are replaced with (8) and (9):

$$\zeta_2 = \frac{m_1 \cdot g}{0.5 \cdot \varrho \cdot \left(v_1 \cdot \frac{D_1^2}{D_2^2} \right)^2 \cdot \frac{\pi}{4} \cdot D_1^2} - \zeta_1 - \left(1 - \left(\frac{D_2}{D_1} \right)^2 \right)^2 \tag{10}$$

With this equation, the pressure loss coefficient of the sample in this specific configuration can be determined.

At this point, a change in setup is required. A new imaginary testing device is needed whose parameters are set to values like the standard EN ISO 9237 uses. The new test environment is required to apply the pressure difference from the EN ISO to the sample in an imaginary test in order to determine the velocities in accordance with EN ISO without any other obstacles in terms of fluid dynamics. So, the new imaginary device is just a pipe with the sample mounted in the pipe, without any steps or other disturbances. As mentioned, Eq. 6 is used again, but with only one pressure loss coefficient, the one from the sample and the pressure difference from EN ISO 9237. Rearranging leads to the velocity perpendicular to the desired value, which is the velocity perpendicular to the sample surface induced by the pressure difference according to the EN ISO 9237. For this purpose, the setup in Figure 8 is used.

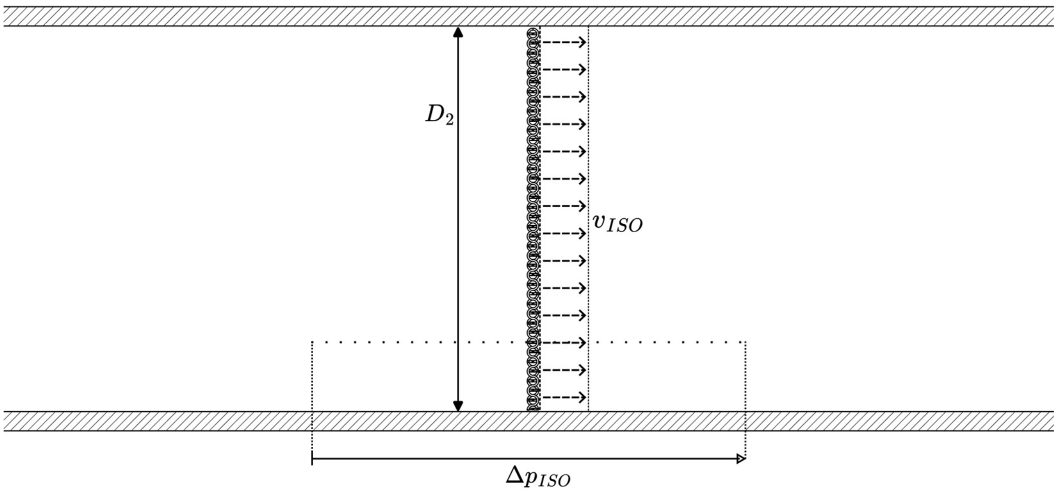

Figure 8. Test setup for calculating the permeability.

The diameter of the effective cross section stays the same as in the testing device before, but the pressure difference is now taken from the EN ISO 9237 ($\Delta p_{ISO} = 100\ \text{Pa}/200\ \text{Pa}$). Again, the Bernoulli equation is used, but this time the only pressure drop coefficient is the one from the sample.

$$\Delta p_{ISO} = \frac{1}{2} \cdot \varrho \cdot v_{ISO}^2 \cdot \zeta_2$$

The value of interest is the velocity v_{ISO} perpendicular to the sample surface which corresponds to the R value from the EN ISO 9237. Rearranging the equation results in the following:

$$v_{ISO} = \sqrt{\frac{\Delta p_{ISO}}{\frac{1}{2} \cdot \varrho \cdot \zeta_2}} \tag{11}$$

The pressure loss coefficient ζ_2 can be replaced by the derived Formula (10), and inserting it into (11) leads to the following:

$$v_{ISO} = \sqrt{\frac{\Delta p_{ISO}}{\frac{1}{2} \cdot \varrho \cdot \left(\frac{m_1 \cdot g}{0.5 \cdot \varrho \cdot \left(v_1 \cdot \frac{D_1^2}{D_2^2} \right)^2 \cdot \frac{\pi}{4} \cdot D_1^2} - \zeta_1 - \left(1 - \left(\frac{D_2}{D_1} \right)^2 \right)^2 \right)}} \tag{12}$$

The result of Equation (12) is the permeability of the sample in meters per second and should give a good first estimation for the comparison of the measured time (here visible in the form of the constant velocity v_1) with the result of a standardized test instrument.

In this calculation, several assumptions have been made which have to be discussed.

As usual, the calculation method, neglecting friction, is only a first attempt to harmonize data or procedures. In the future, it should be tested whether it is possible to adjust the values of the new test device to the values of the standard-compliant test device using simple correction terms in the calculation formula.

Also, the components for the pressure loss coefficient were treated as separate, but due to their spatial proximity they are more likely to be categorized as one component, which means that the calculation may be incorrect.

It should also be checked whether the pressure difference or the flow velocity is in the order of magnitude of the standard-compliant test device. It is not certain whether the pressure difference across the sample increases quadratically with the velocity. There may well be a different correlation, but the error can be minimized by adjusting the speed of the new test device so that the pressure difference from the standard is approximately present. Also, there could be phenomena such as choking, well known from other flow-through components.

To test whether the above equation approximates the measured values of the custom-made test device, Figure 9 depicts theoretical vs. measured values of the air permeability.

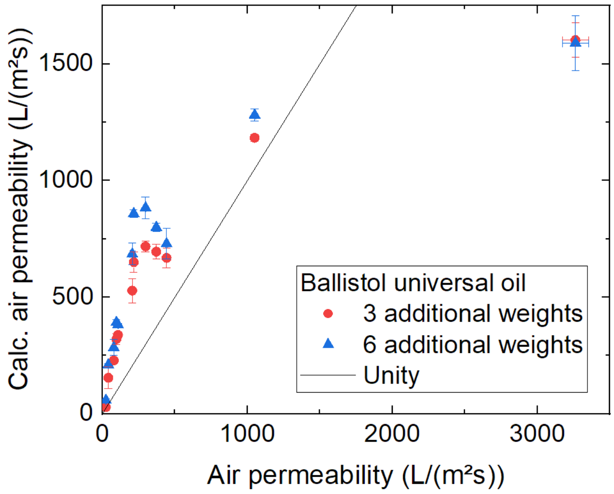

(**a**)

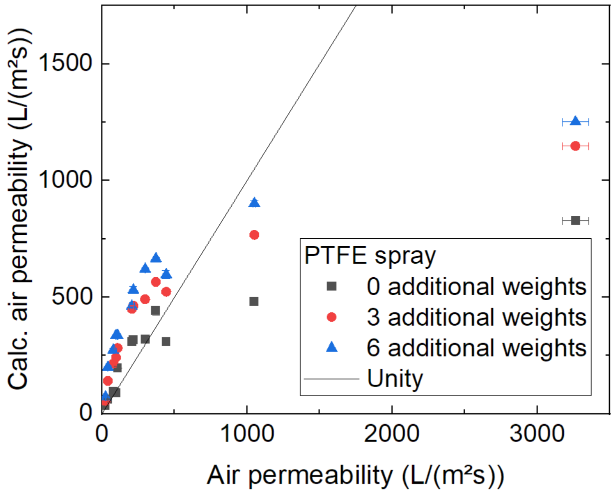

(**b**)

Figure 9. Calculated vs. measured air permeability for (**a**) Ballistol universal oil; (**b**) PTFE spray.

For small values of the air permeability, measurements with Ballistol universal oil give too high calculated air permeability values, while the values calculated from the falling times measured with PTFE spray are similar to those measured with the standardized instrument. For higher air permeabilities, however, the calculated values are in both cases lower than those measured with the standard test procedure. Most importantly, both values are approximately linearly correlated for air permeabilities around 0–500 L/(m^{2}s), allowing a simple conversion by a constant conversion factor. However, there are more measurements needed in the range around 500–3500 L/(m^{2}s) to investigate in which range of value there is a linear correlation, and how higher air permeabilities—where the friction apparently has a larger impact—can be correlated between both measurement methods.

As discussed above, several factors may explain the deviation from the consistency of the values measured with the standardized instrument and those ones calculated from measurements with the custom-made testing instrument. Especially for high air permeability, the velocity of the falling piston is possibly not yet constant. On the other hand, high air permeabilities, such as 3500 L/(m^{2}s), are also near the upper limit of the measurement range of the commercial device, so that here potentially larger errors occur than in a middle range of 10–1000 L/(m^{2}s), in which the automatic measurement range matching stays in one of the middle measurement ranges [16].

While a correlation between both measurements methods has been clearly shown, these deviations necessitate further experiments and simulations of both instruments to investigate correlations and differences more in detail. Furthermore, to improve the repeatability of measurements with such simple air permeability testers produced at different universities or companies, three to five test standards should be defined in the form of masks with defined dimensions and hole geometries, which all researchers can have produced in a simple way in a metal workshop; 3D printed parts should not be used here to avoid the usual dimensional deviations depending on printers, printer settings and printed materials.

5. Conclusions

The air permeability of textile fabrics belongs to the important parameters regarding the comfort and applicability of technical textiles. Since the standardized test instrument is relatively expensive and not easy to build, an alternative test instrument is presented here, based on the principle of a falling piston. Tests series showed that PTFE spray enables the use of less additional weights in the falling piston than Ballistol universal oil. Nevertheless, measurements with more additional weight show less outliers.

A correlation between both measurement principles was calculated, based in simplifying assumptions, which could be fit to the standardized measurements by a multiplication factor for small air permeabilities. For larger air permeabilities, however, the recent calculation needs further modifications to enable direct comparison between both measurement instruments.

Author Contributions: Conceptualization, L.S. and A.E.; methodology, N.R.; software, N.R.; validation, N.R. and A.E.; formal analysis, N.R. and A.E.; investigation, D.S., C.G. and L.S.; writing—original draft preparation, N.R. and A.E.; writing—review and editing, all authors; visualization, D.S., N.R., L.S. and A.E. All authors have read and agreed to the published version of the manuscript.

Funding: This research received no external funding.

Institutional Review Board Statement: Not applicable.

Informed Consent Statement: Not applicable.

Data Availability Statement: All data created during this project are given in the paper.

Conflicts of Interest: The authors declare no conflicts of interest.

References

1. Clayton, F.H. The measurement of the air permeability of fabrics. *J. Text. Inst. Trans.* **1935**, *26*, T171–T186. [CrossRef]
2. Schiefer, H.F.; Boyland, P.M. Improved instrument for measuring the air permeability of fabrics. *J. Res. Natl. Bur. Stand.* **1942**, *28*, 637–642. [CrossRef]
3. Goodings, A.C. Air flow through textile fabrics. *Text. Res. J.* **1964**, *34*, 713–724. [CrossRef]
4. Shen, H.; Xu, Y.F.; Wang, F.M.; Wang, J.L.; Tu, L.X. Numerical analysis of heat and flow transfer in porous textiles–Influence of wind velocity and air permeability. *Int. J. Therm. Sci.* **2020**, *155*, 106432. [CrossRef]
5. Available online: https://www.iso.org/standard/16869.html (accessed on 1 April 2024).
6. Available online: https://www.technormen.de/norm/astm-d737-18_2023-1.6.2023.html (accessed on 1 April 2024).
7. Available online: https://www.techstandardstore.com/product/ASTM-F778-88-2014/ (accessed on 1 April 2024).
8. Tang, X.N.; Jeong, C.-H.; Yan, X. Prediction of sound absorption based on specific airflow resistance and air permeability of textiles. *J. Acoust. Soc. Am.* **2018**, *144*, EL100. [CrossRef] [PubMed]
9. Kim, W.D.; Pyo, S.J.; Kim, M.-O.; Oh, Y.K.; Kwon, D.-S.; Kim, J.B. Humidity-resistant triboelectric energy harvester using electrospun PVDF/PU nanofibers for flexibility and air permeability. *Nanotechnology* **2019**, *30*, 275401. [CrossRef] [PubMed]
10. Khalil, A.; Fouda, A.; Tesinova, P.; Eldeeb, A.S. Comprehensive assessment of the properties of cotton single jersey knitted fabrics produced from different lycra states. *AUTEX Res. J.* **2021**, *21*, 71–78. [CrossRef]
11. Barr, G. The measurement of the porosity of textiles. *J. Text. Inst. Proc.* **1932**, *23*, P206–P213. [CrossRef]
12. Kawabata, S. Method and Apparatus for Measuring Air Permeability of Fiber Material Such as Cloth or Nonwoven Fabric of Every Kind. Patent JPH056133B2, 14 December 1987.
13. Wagner, C.G.; Cain, D.E. Method and Apparatus for Determining Permeability and Thickness of Refractory Coatings on Foundry Molds and Cores. U.S. Patent US4366703A, 4 January 1983.
14. Wang, Y.W.; Pan, J.Q.; Liu, H.Y.; Liu, K.; Huang, F.H.; Niu, S.X.; Cheng, G.Y.; Wang, D.D. Test Equipment Used for Air Circulation Performance of Diesel Soot Particulate Filter. Patent CN108019263A, 11 May 2018.
15. Lyu, L.X.; Daichi, K.; Yang, Y.; Xu, T. Gas Permeability Detecting Device and Determination Method for Tissue Engineering Porous Scaffold. Patent CN106596374A, 26 April 2017.
16. Sabantina, L.; Ehrmann, A. New testing device for air permeability. *Commun. Dev. Assem. Text. Prod.* **2023**, *4*, 164–170. [CrossRef]
17. Bohl, W. *Technische Strömungslehre*, 12th ed.; Vogel: Würzburg, Germany, 2002; ISBN 3-8023-1878-1.